Available online at www.sciencedirect.com
ScienceDirect
Trans. Nonferrous Met. Soc. China 27(2017) 569−577
Transactions of Nonferrous Metals Society of China
www.tnmsc.cn

Role of milling time and Ni content on dehydrogenation behavior of MgH_2/Ni composite

Li-shuai XIE, Jin-shan LI, Tie-bang ZHANG, Hong-chao KOU

State Key Laboratory of Solidification Processing, Northwestern Polytechnical University, Xi'an 710072, China

Received 21 December 2015; accepted 15 June 2016

Abstract: The effects of ball milling time and Ni content on the dehydrogenation performance of MgH_2/Ni composite were systematically investigated. The structural evolution of ball milled MgH_2+x%Ni (x=0, 2, 4, 8, 20, 30, mass fraction) samples during mechanical milling process and dehydrogenation properties were investigated by a series of experimental techniques. The results show that the desorption kinetics is independent of particle size, grain size and defects as the temperature is above 380 °C. The desorption kinetics is improved by prolonged milling time due to refined and uniformly distributed Ni. The formation of Mg_2Ni after dehydrogenation is proposed to explain the degradation of hydrogen storage properties of MgH_2 during de-/hydrogenation cycling process. The desorption activation energy of MgH_2 decreases with the increase of Ni content due to the catalytic effect of Ni. It is found Ni favors the nucleation of magnesium phase and accelerates the recombination of hydrogen atoms.
Key words: magnesium hydride; nickel; nucleation; recombination; high-energy ball milling

1 Introduction

The unique physical and chemical properties of hydrogen make it an outstanding energy carrier in the future out of public concern about environmental pollution and energy depletion [1−3]. The fabrication of safe, efficient and inexpensive hydrogen storage material is the key to hydrogen economy [4]. Magnesium, as well as magnesium-based alloys, is still regarded as one of the most attractive candidates due to its high capacity, low price and high abundance [5]. Nevertheless, the unsatisfactory dehydrogenation temperature of well over 300 °C and sluggish hydrogen desorption rate bring enormous difficulties for its practical applications. The strategies for improving the de-/hydrogenation performance of magnesium mainly include reducing the grain size far below the micrometer scale [6,7], alloying with other elements [8,9] and adding catalytic components [10−12].

In principle, understanding the dehydrogenation steps limiting desorption kinetics can help solve the problems. Unfortunately, attempts to clarify the rate limiting steps by the Johnson−Mehl−Avrami (JMA) equation, which is the most commonly used method for the assessment of the desorption kinetics of magnesium hydrides, have not been fully convincing. The limiting step has been variously suggested as the nucleation and growth of magnesium [13,14], diffusion through the growing layer of the α-phase [15,16] or hydrogen evolution through the surface of the formed metallic islets [17,18]. Apparent experimental evidence of the rate limiting steps is insufficient.

The surface properties, which account for both hydrogen sorption and desorption, can be improved significantly with the addition of catalysts [19]. Although large numbers of papers on magnesium hydrides catalyzed by transition metals, especially nickel, have already been published, the role of transition metals is still ambiguous. The effect of Ni on favoring the recombination of H atoms has been confirmed by both experiments and theoretical calculations [20−22]. JENSEN et al [23] have indicated that the activation energy of Ni catalyzed MgH_2 can be reduced by 50 kJ/mol and Ni preserves little influence on other processes besides the recombination of hydrogen atoms. But the effect of Ni on favoring the nucleation of Mg by weakening Mg—H bond during desorption of MgH_2 is

Foundation item: Project (95-QZ-2014) supported by the Research Fund of the State Key Laboratory of Solidification Processing (NWPU), China; Project supported by the Defense Industrial Technology Development Program, China; Project (B08040) supported by the 111 Program, China
Corresponding author: Tie-bang ZHANG; Tel: +86-29-88491764; Fax: +86-29-88460294; E-mail: tiebangzhang@nwpu.edu.cn
DOI: 10.1016/S1003-6326(17)60063-3

proposed by theoretical calculations [24−26].

Objective experimental evidence of how transition metals improve the kinetics of MgH_2 is still lacking. In the present work, the effects of milling time and Ni content on the dehydrogenation performance of MgH_2/Ni composite are systematically investigated. Meanwhile, the effects of nucleation of Mg phase, hydrogen diffusion and hydrogen recombination on desorption kinetics of MgH_2 are also discussed. It is expected to give objective experimental evidence of Ni on accelerating the nucleation of magnesium phase during desorption of MgH_2.

2 Experimental

2.1 Materials preparation

The raw materials used in the present work were MgH_2 powders (60 μm, containing 2% Mg as impurity) purchased from Alfa Aesar and Ni powders (44 μm, purity: 99.9%) purchased from Acros. Both as-received powders were used without further purification. The MgH_2 powders were pre-milled for 1 h. 4% Ni (mass fraction) was added to the pre-milled MgH_2 powders and then the powders were ball milled for 10, 30, 60 and 120 min, respectively. For each sample, the ball to powder mass ratio was 20:1. Then different amounts of Ni powders were ball milled with pre-milled MgH_2 under the protection of argon for 120 min with the same ball to powder mass ratio. The compositions of the samples were MgH_2+x%Ni (x=0, 2, 4, 8, 20, 30, mass fraction). The mill used in the present study was a vibratory-type high-energy ball mill (Spex 8000D) with a tungsten carbide vial. The balls of 8 or 4 mm in diameter made of stainless steel (SUS316) were employed. All the handing of samples during milling was carried out under purified argon atmosphere in a glove box with an automatic gas purifier unit that maintained low levels of O_2 ($<1\times10^{-6}$) and H_2O ($<1\times10^{-6}$).

2.2 Characterization and measurement

Phase structures of the ball milled powders were characterized by X-ray diffraction (XRD, DX−2700) with Cu K_α radiation, in the 2θ range between 15° and 90°. Diffraction data were collected at room temperature and the voltage and the current were 40 kV and 30 mA, respectively. Rietveld method [27] based on the XRD patterns was used for qualitative and quantitative phase analyses. The full spectrum fitting was carried out to get R value as small as possible before easy quantitative calculations. Scanning electron microscopy (SEM) with a backscattered mode was employed to characterize the microstructure of the powders. The desorption performance of the milled powders was measured by a simultaneous TG-DTA/DSC apparatus (STA449C), which was programmed to heat the specimens at rates of 5, 10 and 15 °C/min up to a maximum temperature of 500 °C.

3 Results and discussion

3.1 Structure characterization

The Rietveld refinements for the XRD patterns of pure MgH_2 milled for 10 min and MgH_2+4%Ni milled for 10, 30, 60 and 120 min are shown in Fig. 1. It is found in Fig. 1(e) that the pure MgH_2 milled for 10 min sample contains dominantly β-MgH_2 together with a certain amount of γ-MgH_2, Mg and MgO. The mass fraction of Mg derived from Rietveld refinement is ~1.8%, close to that of the raw material (~2% Mg as impurity) and the mass fraction of MgO is only ~0.8%, indicating that hydrogen desorption of pure MgH_2 during milling process is not significant. Obvious hydrogen desorption takes place in the MgH_2+4%Ni milled for 10 min sample, which can be derived from the diffraction peaks of magnesium at 32.2°, 34.4° and 36.6° in Fig. 1(a). Thus, it is evident that Ni favors the dehydrogenation of MgH_2.

For MgH_2+4%Ni milled for 10, 30, 60 and 120 min, the full width at half maximum (FWHM) values at 28.01° (2θ) are 0.231°, 0.262°, 0.301° and 0.401°, respectively, indicating that the grain size of β-MgH_2 continually decreases with prolonged milling time estimated from Shcherrer equation [28]. For MgH_2+4%Ni milled for 10, 30, 60 and 120 min, mass fractions of constituent phases are shown in Fig. 2. The mass fraction of γ-MgH_2 increases slightly from 5.2% to 7.0% as the milling time increases from 10 to 120 min. The mass fraction of Ni for each sample is around 4%. No Bragg peaks of Mg_2Ni or Mg_2NiH_4 can be observed in Fig. 1. The mass fraction of Mg decreases with the increase of milling time, contrarily, the content of MgO increases. It is consistent with the changing trend of Bragg diffraction peak (~42.9°) intensities of MgO in Figs. 1(a)−(d). The fresh surface of magnesium produced from dehydrogenation of magnesium hydrides with the help of nickel is gradually oxidized. For the four samples, each sample's total mass fraction of Mg and MgO is around 10%, indicating that magnesium is no longer produced after milling for 10 min.

The desorbed hydrogen from MgH_2 in the vial during ball milling process may impede the further dehydrogenation of MgH_2. To confirm this, another experiment was designed. For MgH_2+4%Ni, after it had been milled for 10 min, the vial was re-filled with high purity argon in glove box, and then it was milled for another 20 min. For convenience, it is denoted as MgH_2+ 4%Ni milled for (10+20) min. The XRD pattern is displayed in Fig. 1(f). The diffraction peaks of

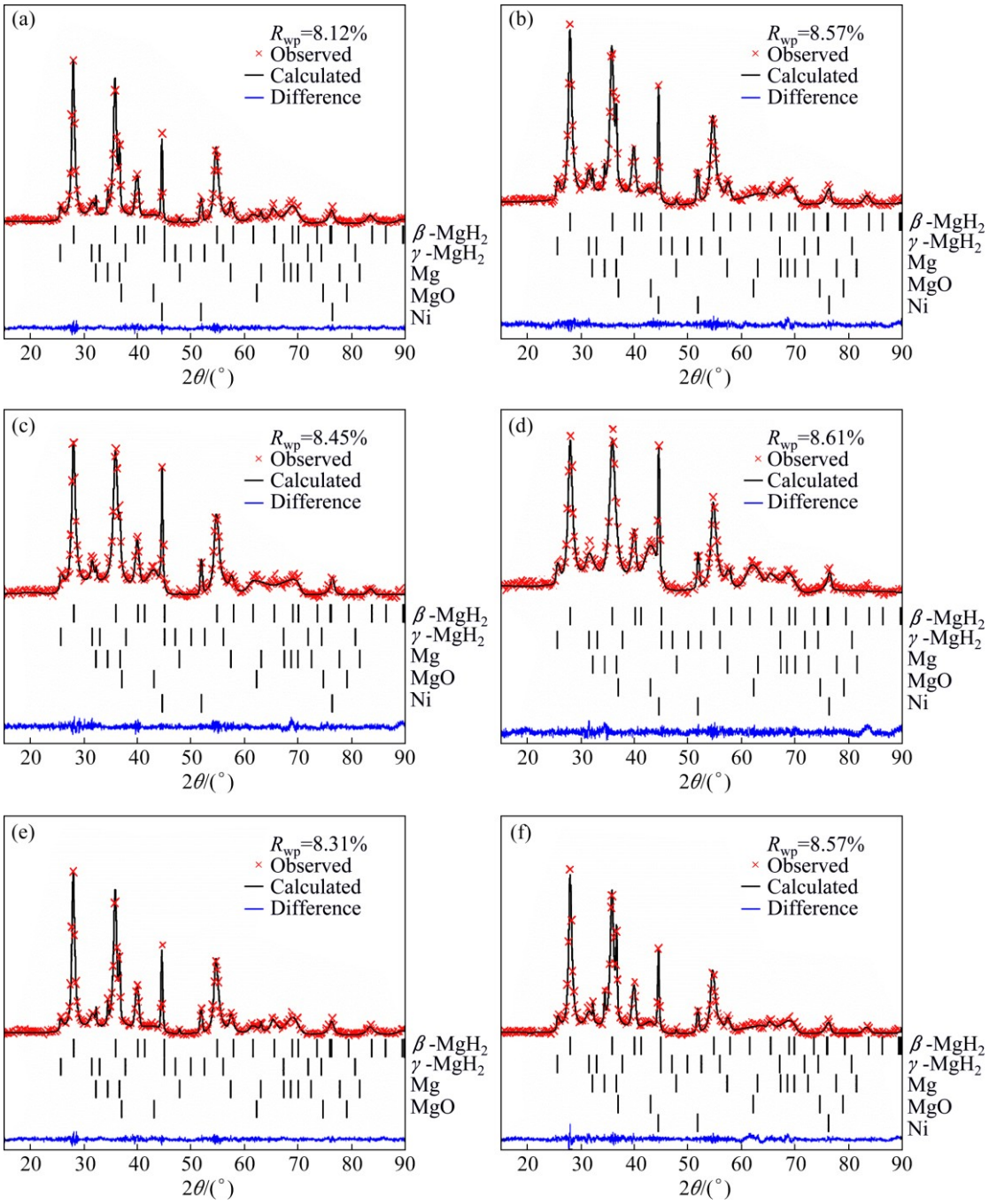

Fig. 1 Rietveld refinements for XRD patterns of MgH_2+4%Ni milled for 10 min (a), 30 min (b), 60 min (c), 120 min (d) and pure MgH_2 milled for 10 min (e) and MgH_2+4%Ni milled for (10+20) min (f)

magnesium at 32.2°, 34.4° and 36.6° imply that much more Mg has been obtained. The mass fraction of Mg, significantly higher than those of MgH_2+4%Ni milled for 30 min and MgH_2+4%Ni milled for 10 min, is ~13.1%. The mass fraction of MgO is close to that of MgH_2+4%Ni milled for 30 min. It is logical to conclude that the desorbed hydrogen from MgH_2 during milling assuredly impedes the further desorption of MgH_2. The oxides can also prevent the further dehydrogenation of MgH_2.

Figure 3 shows the SEM/BSE images of MgH_2+4%Ni milled for various time. With prolonged milling time, large MgH_2 particles are pulverized into smaller ones, meanwhile, nickel particles (average 44 μm in diameter used as raw material) are also pulverized and distribute on the surface of magnesium hydrides more uniformly. More MgH_2 powders are covered with Ni with prolonged milling time. Due to short milling time (no more than 120 min) and micro-Ni particles used as raw material in the present experiment, nickel powders do not distribute on each MgH_2 powder's surface for the four samples.

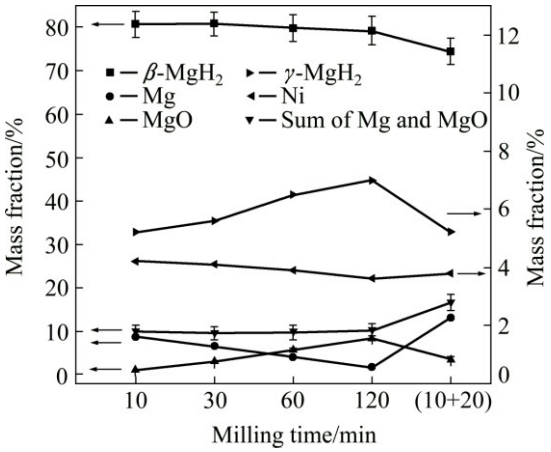

Fig. 2 Mass fractions of constituent phases of MgH_2+4%Ni with various milling time

3.2 Hydrogen desorption of ball-milled MgH_2

The DSC and TGA curves of MgH_2+4%Ni milled for various time are illustrated in Figs. 4(a) and (b), respectively. There are three endothermic peaks for each sample. As discussed earlier, fragmentized Ni cannot distribute on each MgH_2 particle's surface. For each sample, the peak at temperature above 380 °C corresponds to the dehydrogenation of MgH_2 uncovered with Ni and the peak in the temperature range from 300 to 380 °C corresponds to the dehydrogenation of Ni catalyzed β-MgH_2. The peak at temperature below 300 °C can be ascribed to the dehydrogenation of Ni catalyzed γ-MgH_2 [29]. For each sample, the peak at temperature above 380 °C locates around 420 °C. The onset temperature and peak temperature of peaks at temperature below 380 °C show a downward trend with prolonged milling time.

As illustrated in the TGA curves, there are two dehydrogenation stages of each sample and the critical temperature is around 380 °C, which is consistent with DSC results. The second stage (at temperature above 380 °C) corresponds to the dehydrogenation of MgH_2 powders which are not catalyzed by Ni and the first stage (at temperature below 380 °C) corresponds to the dehydrogenation of Ni catalyzed MgH_2. For each sample, the total amount of desorbed hydrogen from the TGA measurement is about 6.3%. For the second stage, MgH_2+4%Ni milled for 10, 30 and 60 min shares a similar hydrogen desorption rate indicated by the slope of the mass loss vs temperature curve. For MgH_2+4%Ni milled for 120 min, it mostly releases hydrogen at temperature below 350 °C and there is a bit of inevitable oxidation at high temperature.

With increasing milling time, both grain size and particle size decrease, which can be seen from the XRD results and SEM images. It is commonly accepted that longer milling time brings more defects and the defects favor the nucleation of magnesium and diffusion of hydrogen atoms. The decreased grain size and particle size can shorten the diffusion distance of hydrogen atoms. But no desorption discrepancy at temperature above 380 °C is observed from DSC and TGA curves of MgH_2+4%Ni milled for various time. In other words, the

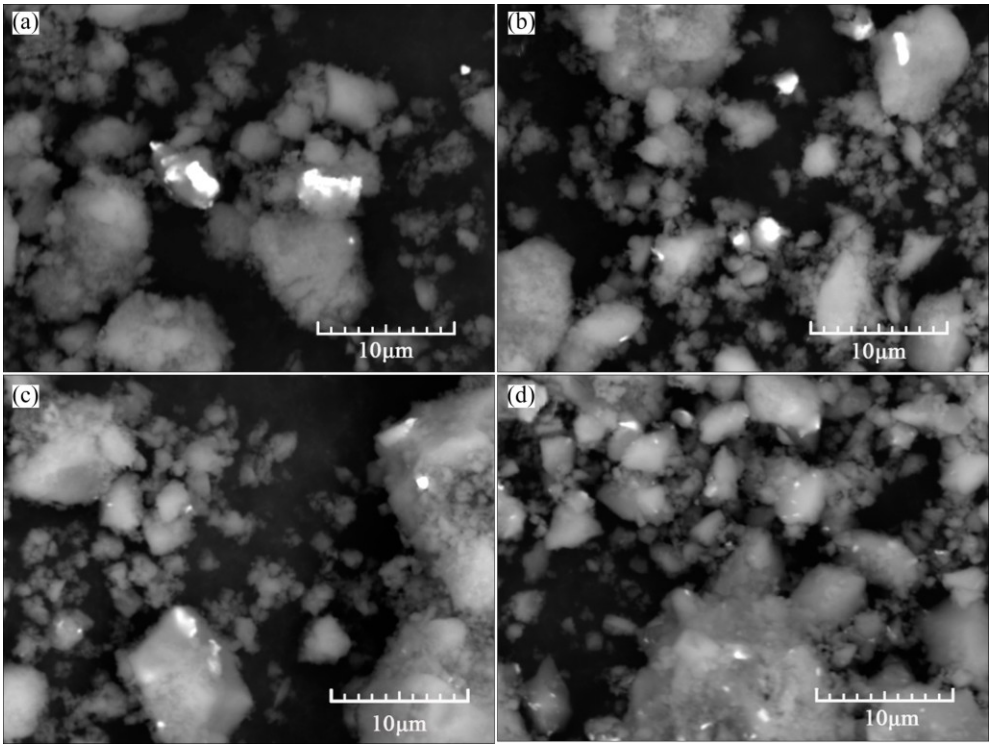

Fig. 3 SEM/BSE images of MgH_2+4%Ni milled for various time: (a) 10 min; (b) 30 min; (c) 60 min; (d) 120 min

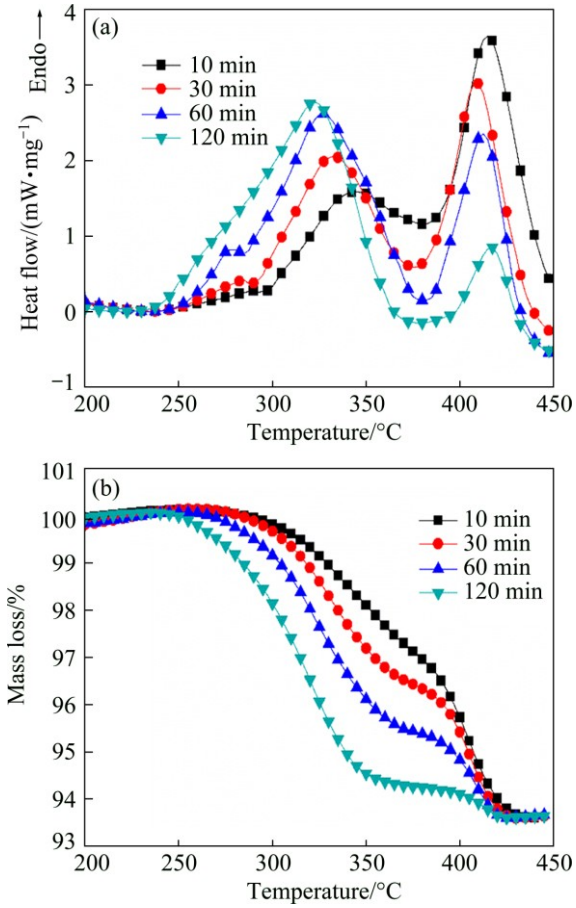

Fig. 4 DSC curves (a) and TGA curves (b) for MgH_2+4%Ni milled for 10, 30, 60 and 120 min at heating rate of 10 °C/min with argon flow

dehydrogenation kinetics is independent of particle size, grain size and the amount of defects at temperature above 380 °C. Therefore, the desorption kinetics are not limited by nucleation and growth of magnesium and hydrogen diffusion at temperature above 380 °C, and the limiting step is probably the recombination of hydrogen atoms. XIE et al [30] have found that the activation energy of desorption under hydrogen atmosphere is much larger than that under argon atmosphere, indicating that the recombination of hydrogen atoms limits the desorption process considerably [30]. EVARD et al [17] have also found that hydrogen evolution from magnesium surface is a desorption-limited process by physically justified models. In the present work, the dehydrogenation of MgH_2 stops as a certain amount of hydrogen is generated in the vial during the milling process. Now that the recombination of hydrogen atoms is a thermal activation process, more strategies are needed to overcome the recombination barrier of desorption at lower temperature.

HUOT et al [31] have proven that high-energy milling does not change the thermodynamic properties of magnesium hydrides. But it modifies the kinetic properties significantly. With the increase of milling time, the onset desorption temperature decreases and the kinetics improves, which can be seen from DSC and TGA curves at temperature below 380 °C, although there are more oxides. MgO is always regarded as a barrier between MgH_2 and hydrogen due to its dense rock-salt structure limiting the diffusion of hydrogen atoms [23]. Longer milling time refines Ni and makes Ni distribute on the surface of MgH_2 more uniformly and brings faster desorption kinetics. The efficiency of Ni largely depends on its site density over MgH_2 surface. Decreased particle size, grain size and increased defects induced from longer milling time also contribute the faster kinetics at temperature below 380 °C [32].

XRD patterns of MgH_2+4%Ni milled for 120 min which has been heated to 380 °C (only after the first stage dehydrogenation) and 500 °C (after full dehydrogenation) are shown in Figs. 5(a) and (b), respectively. From Fig. 5(a), Bragg peaks of β-MgH_2 appear around 28° and 54.6°, and Mg and MgO can still be clearly observed. Bragg peaks of γ-MgH_2 disappear, but obvious Bragg peaks of Mg_2Ni arise and intensities of Bragg peaks from Ni decrease significantly, indicating that most of Ni has reacted with Mg to form Mg_2Ni.

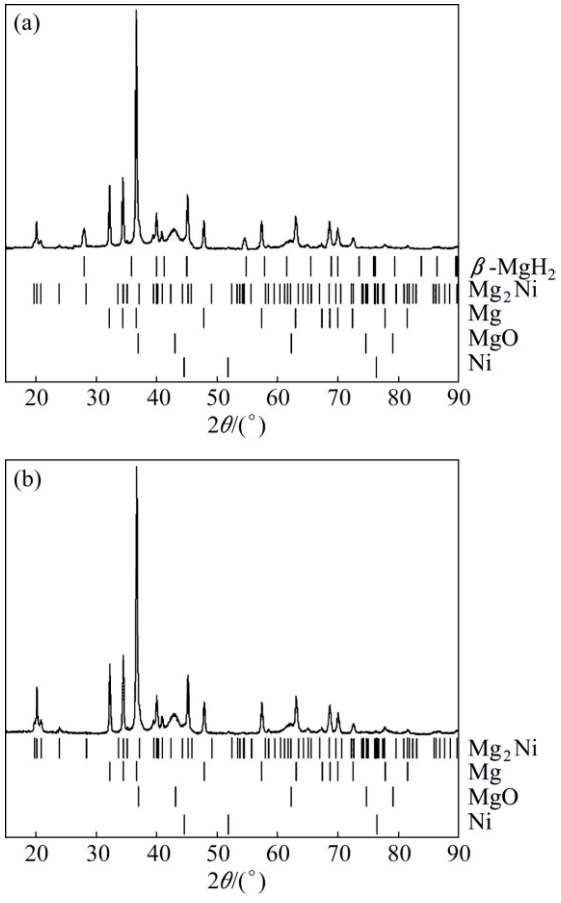

Fig. 5 XRD patterns of MgH_2+4%Ni milled for 120 min after first stage dehydrogenation (a) and after full dehydrogenation (b)

In Fig. 5(b), Bragg peaks of Mg_2Ni can still be clearly observed and Bragg peaks of β-MgH_2 disappear.

According to the DSC/TGA curves in Fig. 4 and XRD patterns in Fig. 5, it is reasonable to conclude the reactions taking place in Ni catalyzed MgH_2 during heating. Firstly, MgH_2 particles catalyzed by Ni desorb and the generated Mg reacts with Ni to form Mg_2Ni (at temperature below 380 °C). Then, the remaining MgH_2 desorbs at higher temperature accompanied by the reaction between Mg and remaining metallic Ni (if any).

The results coincide well with the work of LIANG et al [33] and KWON et al [34]. A complete transformation of Ni observed in the XRD spectrum of ball milled MgH_2−5%Ni composite after dehydrogenation at 300 °C has been found by LIANG et al [33]. Catalytic effect of Mg_2Ni on dehydrogenation of MgH_2 is relatively weak.

Based on the above results, ball milling pre-refined MgH_2 powders and Ni powders for a short period of time can produce better desorption performance. It can reduce the oxidation of Mg and avoid the formation of Mg_2NiH_4 [31,33]. Reducing the chance of direct contact of Ni and MgH_2 is probably an effective method to improve the cycling stability, such as loading the catalyst in other carriers.

3.3 Catalytic effect of Ni on Mg nucleation during dehydrogenation

The XRD results and SEM/BSE images of MgH_2+x%Ni milled for 120 min are shown in Figs. 6 and 7, respectively. All the samples are composed of β-MgH_2, γ-MgH_2, MgO, Mg and Ni. The full width at half maximum values of the samples at 28.01° are in the range of 0.401° to 0.4013°, indicating that the grain sizes of β-MgH_2 are almost the same estimated from Shcherrer equation [28]. Figure 7 displays the distribution of Ni on the surface of MgH_2. For MgH_2+4%Ni milled for 120 min, partial MgH_2 powders are not covered with Ni. Few MgH_2 powders are uncovered with Ni for MgH_2+20%Ni milled for 120 min.

The DSC/TGA curves of MgH_2+x%Ni (x=0, 2, 4, 8, 20, 30) are shown in Figs. 8(a) and (b), respectively. Each sample has two endothermic peaks. Accordingly, there are two stages in TGA curves. For MgH_2+4%Ni and MgH_2+8%Ni samples, the quantities of desorbed hydrogen are extremely close, which can be ascribed to the experimental error and the inevitable oxidation at high temperature. It can be clearly observed from TGA curves in Fig. 8(b) that the mass of each sample increases slightly at temperature above 430 °C due to the partial oxidation of Mg. In DSC curves, the intensities of peaks at higher temperature decrease with the increase of Ni content. The peaks at higher temperature have identical peak temperature with pure MgH_2, which have been

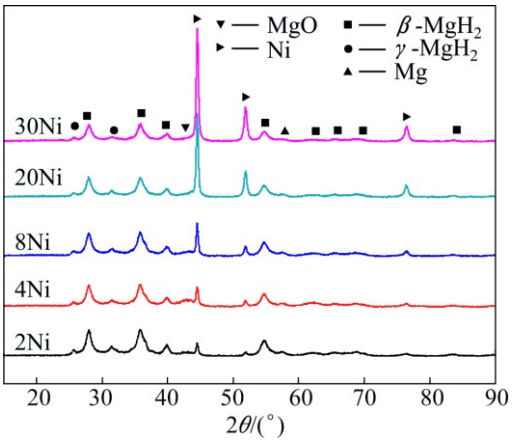

Fig. 6 XRD patterns of MgH_2+x%Ni (x=2, 4, 8, 20, 30) milled for 120 min

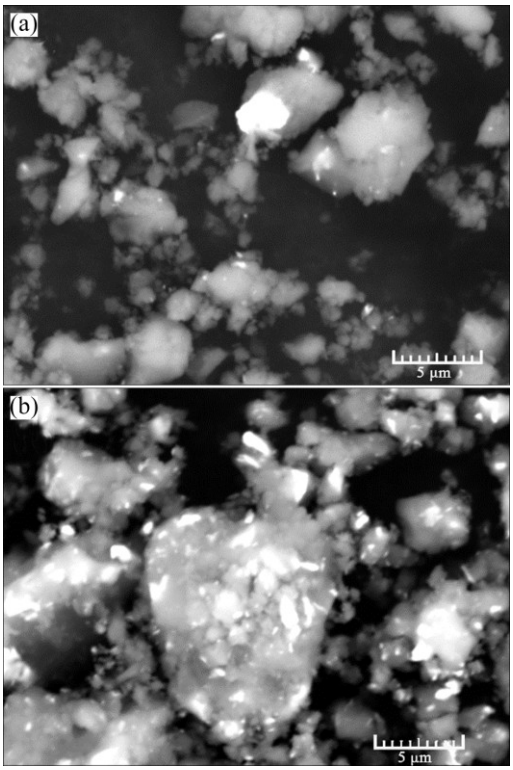

Fig. 7 SEM/BSE images of MgH_2+4%Ni (a), MgH_2+20%Ni (b) milled for 120 min, showing distribution of Ni on surface of MgH_2

milled for the same time with Ni doped MgH_2, giving the evidence that the peaks at higher temperature correspond to the desorption of MgH_2 which are not covered with Ni. With the increase of Ni content, more MgH_2 powders are catalyzed. The onset temperature and peak temperature of peaks at lower temperature have a manifest downtrend and faster kinetics is achieved when increasing the amount of Ni.

DSC tests at different heating rates have been also performed to determine the desorption activation energy

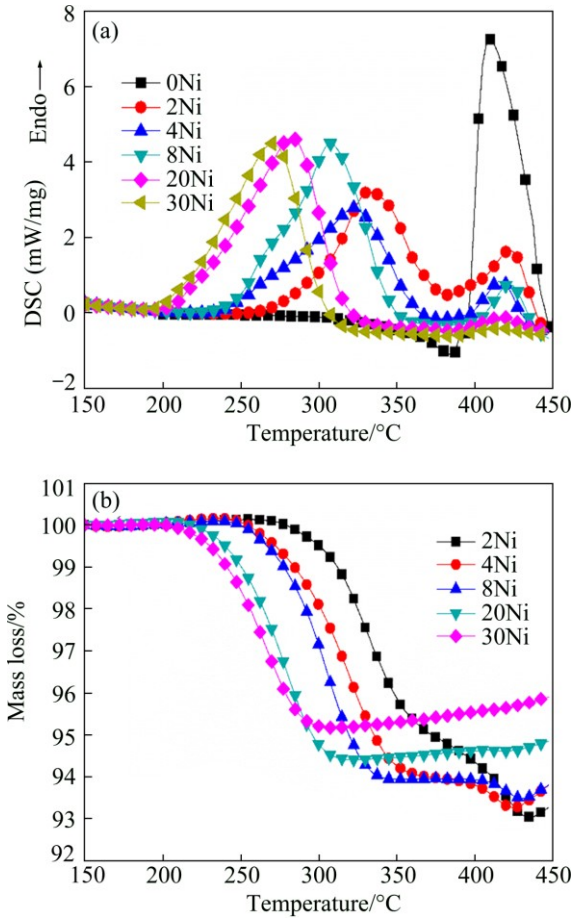

Fig. 8 DSC curves (a) and TGA curves (b) of MgH_2+x%Ni (x=0, 2, 4, 8, 20, 30) at heating rate of 10 °C/min with argon flow

of MgH_2. The activation energy is calculated using Kissinger equation [35]:

$$\frac{\mathrm{d}(\ln\beta / T_\mathrm{p}^2)}{\mathrm{d}(1/T_\mathrm{p})} = -\frac{E_\mathrm{A}}{R} \quad (1)$$

where T_p is the peak temperature, β is the heating rate, E_A is the activation energy and R is the gas constant. The plot of $\ln(\beta/T_\mathrm{p}^2)$ versus $1000/T_\mathrm{p}$ is shown in Fig. 9. The activation energy of each sample is obtained from the slope of the fitted line, as shown in Table 1.

The desorption activation energy of pure MgH_2 after being milled for 120 min is 168 kJ/mol. With the increase of Ni content, the activation energy decreases. The activation energy of desorption is 83 kJ/mol for MgH_2+30%Ni. It is generally accepted that Mg does not promote dissociation of hydrogen molecular and recombination of hydrogen atoms on its surface. The activation energy of hydrogen dissociation on Mg surface is about 50 kJ/mol, which is approved by both experiments and theoretical calculations [22]. In contrast, nickel is recognized to assist the recombination of hydrogen atoms significantly, i.e., recombination of hydrogen atoms on Ni preserves a negligible activation barrier around 10 kJ/mol [23,36]. The experimentally observed difference in E_A for the desorption of pure MgH_2 and MgH_2+30%Ni (168 kJ/mol and 83 kJ/mol, respectively) is 85 kJ/mol, which is greater than the activation energy of hydrogen recombination on Mg surface.

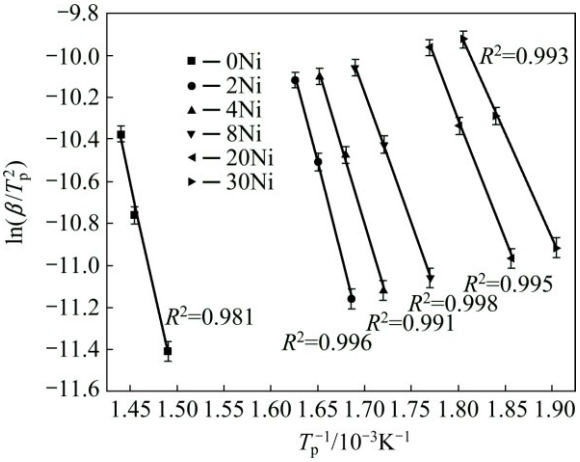

Fig. 9 Plot of $\ln(\beta/T_\mathrm{p}^2)$ versus $1000/T_\mathrm{p}$ of MgH_2+x%Ni (x=0, 2, 4, 8, 20, 30)

Table 1 Peak temperature, onset temperature from DSC results, onset temperature from TGA curves and activation energy of desorption

Ni content/ %	Peak temperature of desorption/ °C	Onset temperature of desorption/ °C	Activation energy/ (kJ·mol^{-1})	Onset temperature from TG curves/°C
0	415	374	168	–
2	333	236	144	264
4	322	222	124	246
8	308	216	104	236
20	282	191	95	210
30	270	186	83	201

The release of hydrogen from MgH_2 begins with the nucleation of HCP-Mg phase followed by the diffusion and recombination of hydrogen atoms [37]. The first step is of prime importance, because it determines whether there are unengaged hydrogen atoms. The onset temperature of DSC peak and onset temperature of TGA curve is not synchronized. As shown in Table 1, the onset temperature of DSC peak is always lower than that of TGA curve. It is well known that DSC peaks reflect the thermal changes, but TGA curves reflect the mass changes. The difference of the onset temperature of DSC peak and TGA curve indicates a nucleation time and diffusion process prior to the initial desorption of hydrogen molecules, which is consistent with the results obtained by in situ time-resolved powder X-ray

diffraction [23]. The difference decreases when increasing the amount of Ni. In other words, Ni shortens the nucleation time of Mg during desorption of MgH_2. Considering the difference in activation energy between pure MgH_2 and MgH_2+30%Ni, it can be inferred that Ni favors the nucleation and growth of magnesium phase. The promotion is obvious only when the Ni content is high.

4 Conclusions

1) The effects of milling time and Ni content on the desorption performance of MgH_2 are systematically studied. The structure, morphology and the dehydrogenation performance of ball milled MgH_2+ x%Ni (x=0, 2, 4, 8, 20, 30) are investigated. The desorption kinetics is independent of particle size, grain size and the defects when the temperature is above 380 °C, indicating that the desorption kinetics is independent of nucleation of Mg phase and diffusion of hydrogen at temperature above 380 °C. Recombination of hydrogen atoms limits the desorption process considerably.

2) The desorption kinetics is improved by prolonged milling time due to refined and uniformly distributed Ni. The formation of Mg_2Ni after dehydrogenation is proposed to explain the degradation of hydrogen storage properties.

3) The activation energy decreases with the increase of Ni content. Ni favors the nucleation of magnesium phase and accelerates the recombination of hydrogen atoms.

References

[1] DAVID E. An overview of advanced materials for hydrogen storage [J]. Journal of Materials Processing Technology, 2005, 162−163: 169−177.

[2] JAIN I P, LAL C, JAIN A. Hydrogen storage in Mg: A most promising material [J]. International Journal of Hydrogen Energy, 2010, 35(10): 5133−5144.

[3] JAIN I P. Hydrogen the fuel for 21st century [J]. International Journal of Hydrogen Energy, 2009, 34(17): 7368−7378.

[4] SAKINTUNA B, LAMARIDARKRIM F, HIRSCHER M. Metal hydride materials for solid hydrogen storage: A review [J]. International Journal of Hydrogen Energy, 2007, 32(9): 1121−1140.

[5] ZHOU C, FANG Z Z, SUN P. An experimental survey of additives for improving dehydrogenation properties of magnesium hydride [J]. Journal of Power Sources, 2015, 278: 38−42.

[6] PHETSINORATH S, ZOU J X, ZENG X Q, SUN H Q, DING W J. Preparation and hydrogen storage properties of ultrafine pure Mg and Mg−Ti particles [J]. Transactions of Nonferrous Metals Society of China, 2012, 22(8): 1849−1854.

[7] HOUSE S D, VAJO J J, REN C, ROCKETT A A, ROBERTSON I M. Effect of ball-milling duration and dehydrogenation on the morphology, microstructure and catalyst dispersion in Ni-catalyzed MgH_2 hydrogen storage materials [J]. Acta Materialia, 2015, 86: 55−68.

[8] SONG W J, LI J S, ZHANG T B, HOU X J, KOU H C, XUE X Y, HU R. Microstructure and hydrogenation kinetics of Mg_2Ni-based alloys with addition of Nd, Zn and Ti [J]. Transactions of Nonferrous Metals Society of China, 2013, 23(12): 3677−3684.

[9] WU Y, XING N, LU Z C, HAN W, ZHOU S X, SOLBERG J K, YARTYS V A. Microstructural evolution of melt-spun Mg−10Ni−2Mm hydrogen storage alloy [J]. Transactions of Nonferrous Metals Society of China, 2011, 21(1): 121−126.

[10] XU C C, XIAO X Z, SHAO J, LIU L X, QIN T, CHEN L X. Effects of Ti-based additives on Mg_2FeH_6 dehydrogenation properties [J]. Transactions of Nonferrous Metals Society of China, 2016, 26(3): 791−798.

[11] LI J J, ZHOU J F, ZHAO X Y, YANG M, MA L Q, SHEN X D. Electrochemical hydrogen storage properties of non-equilibrium $Ti_{2-x}Mg_xNi$ alloys [J]. Transactions of Nonferrous Metals Society of China, 2015, 25(11): 3729−3735.

[12] KWAK Y J, LEE S H, MUMM D R, SONG M Y. Development of a Mg-based hydrogen-storage material by addition of Ni and NbF_5 via milling under hydrogen [J]. International Journal of Hydrogen Energy, 2015, 40(35): 11908−11916.

[13] DAL T S, LO RUSSO S, MADDALENA A, PRINCIPI G, SABER A, SARTORI S, SPATARU T. Hydrogen desorption from magnesium hydride–graphite nanocomposites produced by ball milling [J]. Materials Science and Engineering B, 2004, 108(1−2): 24−27.

[14] BOHMHAMMEL K, CHRIST B, WOLF G. Kinetic investigations on the basis of isothermal DSC measurements of hydrogenation and dehydrogenation of magnesium hydride [J]. Thermochimica Acta, 1998, 310(1−2): 167−171.

[15] CHERNOV I, BLOCH J, VOIT A, GABIS I. Influence of metal powder particle's shape on the kinetics of hydriding [J]. International Journal of Hydrogen Energy, 2010, 35(1): 253−258.

[16] CHEN C Y, CHEN H L, MA Y Q, LIU J. Hydrogen desorption kinetics mechanism of Mg−Ni hydride under isothermal and non-isothermal conditions [J]. Transactions of Nonferrous Metals Society of China, 2016, 26(1): 160−166.

[17] EVARD E, GABIS I, YARTYS V A. Kinetics of hydrogen evolution from MgH_2: Experimental studies, mechanism and modelling [J]. International Journal of Hydrogen Energy, 2010, 35(17): 9060−9069.

[18] HANADA N, ICHIKAWA T, FUJII H. Catalytic effect of nanoparticle 3d-transition metals on hydrogen storage properties in magnesium hydride MgH_2 prepared by mechanical milling [J]. J Phys Chem B, 2005, 109(15): 7188−7194.

[19] WEBB C J. A review of catalyst-enhanced magnesium hydride as a hydrogen storage material [J]. Journal of Physics and Chemistry of Solids, 2015, 84: 96−106.

[20] LIU T, WANG C, WU Y. Mg-based nanocomposites with improved hydrogen storage performances [J]. International Journal of Hydrogen Energy, 2014, 39(26): 14262−14274.

[21] POZZO M, ALF D. Hydrogen dissociation and diffusion on transition metal (= Ti, Zr, V, Fe, Ru, Co, Rh, Ni, Pd, Cu, Ag)-doped Mg(0001) surfaces [J]. International Journal of Hydrogen Energy, 2009, 34(4): 1922−1930.

[22] SPRUNGER P T, PLUMMER E W. An experimental study of the interaction of hydrogen with the Mg(0001) surface [J]. Chem Phys Lett, 1991, 187(6): 559−564.

[23] JENSEN T, ANDREASEN A, VEGGE T, ANDREASEN J, STAHL K, PEDERSEN A, NIELSEN M, MOLENBROEK A, BESENBACHER F. Dehydrogenation kinetics of pure and nickel-doped magnesium hydride investigated by in situ time-resolved powder X-ray diffraction [J]. International Journal of Hydrogen Energy, 2006, 31(14): 2052−2062.

[24] LARSSON P, ARAUJO C M, LARSSON J A, JENA P, AHUJA R. Role of catalysts in dehydrogenation of MgH_2 nanoclusters [J]. Proceedings of the National Academy of Sciences of the United

States of America, 2008, 105(24): 8227−8231.
[25] GIUSEPPONI S, CELINO M. The role of nickel catalyst in hydrogen desorption from MgH_2: A DFT study [J]. International Journal of Hydrogen Energy, 2015, 40(30): 9326−9334.
[26] ZHAO S, XU B, SUN N, SUN Z, ZENG Y, MENG L. Improvement in dehydrogenation performance of $Mg(BH_4)_2{\cdot}2NH_3$ doped with transition metal: First-principles investigation [J]. International Journal of Hydrogen Energy, 2015, 40(28): 8721−8731.
[27] RIETVELD H M. A profile refinement method for nuclear and magnetic structures [J]. J Appl Crystallogr, 1969, 2: 65−70.
[28] BALZAR D, AUDEBRAND N, DAYMOND M R, FITCH A, HEWAT A, LANGFORD J I, LE BAIL A, LOUER D, MASSON O, MCCOWAN C N, POPA N C, STEPHENS P W, TOBY B H. Size-strain line-broadening analysis of the ceria round-robin sample [J]. J Appl Crystallogr, 2004, 37: 911−924.
[29] DENYS R V, RIABOV A B, MAEHLEN J P, LOTOTSKY M V, SOLBERG J K, YARTYS V A. In situ synchrotron X-ray diffraction studies of hydrogen desorption and absorption properties of Mg and Mg−Mm−Ni after reactive ball milling in hydrogen [J]. Acta Materialia, 2009, 57(13): 3989−4000.
[30] XIE L, LIU Y, WANG Y T, ZHENG J, LI X G. Superior hydrogen storage kinetics of MgH_2 nanoparticles doped with TiF_3 [J]. Acta Materialia, 2007, 55(13): 4585−4591.
[31] HUOT J, LIANG G, SCHULZ R. Mechanically alloyed metal hydride systems [J]. Applied Physics A−Materials Science & Processing, 2001, 72(2): 187−195.
[32] AGUEY-ZINSOU K F, ARES FERNANDEZ J R, KLASSEN T, BORMANN R. Effect of Nb_2O_5 on MgH_2 properties during mechanical milling [J]. International Journal of Hydrogen Energy, 2007, 32(13): 2400−2407.
[33] LIANG G, HUOT J, BOILY S, van NESTE A, SCHULZ R. Catalytic effect of transition metals on hydrogen sorption in nanocrystalline ball milled MgH_2−Tm (Tm=Ti, V, Mn, Fe and Ni) systems [J]. Journal of Alloys and Compounds, 1999, 292(1-2): 247−252.
[34] KWON S, MUMM D, PARK H, SONG M. Effects of transition metal oxide and Ni addition on the hydrogen-storage properties of Mg [J]. J Mater Sci, 2010, 45(19): 5164−5170.
[35] KISSINGER H E. Reaction kinetics in differential thermal analysis [J]. Anal Chem, 1957, 29(11): 1702−1706.
[36] FREY G D, LAVALLO V, DONNADIEU B, SCHOELLER W W, BERTRAND G. Facile splitting of hydrogen and ammonia by nucleophilic activation at a single carbon center [J]. Science, 2007, 316(5823): 439−441.
[37] TANNIRU M, TIEN H Y, EBRAHIMI F. Study of the dehydrogenation behavior of magnesium hydride [J]. Scripta Materialia, 2010, 63(1): 58−60.

球磨时间及镍含量对 MgH_2/Ni 复合体系放氢性能的影响

解立帅，李金山，张铁邦，寇宏超

西北工业大学 凝固技术国家重点实验室，西安 710072

摘　要：通过对 MgH_2+x%Ni (x=0, 2, 4, 8, 20, 30)样品高能球磨不同时间，研究球磨时间及镍含量对 MgH_2/Ni 体系放氢性能的影响。对合金在球磨过程中的结构变化、组织演变及放氢动力学进行了系统研究。结果表明，当放氢温度高于 380 °C 时，MgH_2 的放氢动力学与晶粒尺寸、颗粒尺寸及合金中的缺陷数量无关，随着球磨时间增加，镍在 MgH_2 表面分布更加均匀，放氢动力学性能越好。体系放氢后会生成 Mg_2Ni，从而降低复合体系在循环过程中的储氢性能。在 MgH_2 放氢过程中，镍不仅有助于氢原子的重组，还可以帮助镁的形核长大。

关键词：氢化镁；镍；形核；重组；高能球磨

(Edited by Yun-bin HE)